The Astrophysical Journal, 686: L33–L36, 2008 October 10

THE SOLAR WIND POWER FROM MAGNETIC FLUX

N. A. Schwadron[1,2] and D. J. McComas[2]
Received 2008 July 31; accepted 2008 August 28; published 2008 September 16

ABSTRACT

Observations of the fast, high-latitude solar wind throughout *Ulysses*' three orbits show that solar wind power correlates remarkably well with the Sun's total open magnetic flux. These observations support a recent model of the solar wind energy and particle sources, where magnetic flux emergence naturally leads to an energy flux proportional to the strength of the large-scale magnetic field. This model has also been shown to be consistent with X-ray observations of the Sun and a variety of other stars over 12 decades of magnetic flux. The observations reported here show that the Sun delivers ~600 kW Wb^{-1} to power the solar wind, and that this power to magnetic flux relation has been extremely stable over the last 15 years. Thus, the same law that governs energy released in the corona and from other stars also applies to the total energy in the solar wind.

Subject heading: solar wind

1. INTRODUCTION

In 1990 October, the launch of *Ulysses* began a scientific journey of remarkable discovery. After swinging by Jupiter in 1992 February, *Ulysses*' first polar orbit took it over high northern and southern solar latitudes near solar minimum, and *Ulysses* discovered the global 3D structure of the solar wind (McComas et al. 1998, 2000) in solar cycle 22. The solar minimum configuration showed the steady fast solar wind (~750 km s^{-1}) from the Sun's large, dark coronal holes near its poles. The Sun's open magnetic flux is dragged out by the solar wind to fill the heliosphere. The coronal holes are the dominant sources of open flux, and during solar minimum, the open flux is unipolar in each coronal hole, but with opposite polarities. As dictated by the conservation of magnetic flux, the total open flux of the northern polar coronal hole, which had positive polarity in solar cycle 22, is almost exactly compensated by the oppositely directed open flux from the southern polar coronal hole. Any small lack of magnetic flux balance between the northern and southern coronal holes is compensated by open magnetic flux from outside these coronal holes.

The second orbit of *Ulysses* took it through a very different 3D heliosphere during the reconfiguration of the Sun's solar wind and the open field near solar maximum (McComas et al. 2003). As the Sun evolves from one solar minimum to the next, it must entirely reverse the open fields of the Sun, swapping the inward and outward open flux between the two poles for the next solar minimum. While there is no agreement about how this reconfiguration is achieved (e.g., Babcock 1961; Fisk & Schwadron 2001; Owens et al. 2007), the *Ulysses* observations and remote observations of the Sun near solar maximum reveal the breakdown of the well-ordered solar minimum structure. The solar maximum Sun does not have its open magnetic flux organized simply in large polar coronal holes. Instead, small coronal holes of both polarities appear at all latitudes. Similarly, *Ulysses* observed regions of fast and slow solar wind at all latitudes, and the heliospheric current sheet, which separates the oppositely polarized field on large scales, became highly inclined and distorted (Smith & Balogh 2003) as the open field reversed.

The reconfiguration of the open field has been the subject of active research. One suggestion is that open flux is approximately conserved and its reversal is achieved through its massive reorganization on the Sun (Fisk & Schwadron 2001; Owens et al. 2007; Schwadron et al. 2008). This is consistent with the breakdown of polar coronal holes as activity increases, and then the reordering of polar coronal holes with opposite polarity as activity declines into a new solar minimum. The conservation of open flux is also consistent with a reported floor in the level of the interplanetary magnetic field derived from its long-term (~130 years) reconstruction based on geomagnetic indices (Svalgaard & Cliver 2007). However, Wang et al. (2002) point out that the reorganization of open magnetic flux can be predicted on the basis of source surface models (Schatten et al. 1969), which simply use solar magnetograms as input. By examining the results of these models, it appears that the open flux is not reorganized, but actually destroyed through reconnection of oppositely oriented field lines beneath the Alfvén point (~15 $R_\odot$) and reinstated with the release of coronal mass ejections that introduce new open magnetic flux with the opposite polarity. If this were correct, it should be possible for the level of open flux to change from one solar cycle to the next. Indeed, the magnetic field observed by *Ulysses* in the new fast wind of solar minimum is lower by ~25% compared to the previous minimum (Smith & Balogh 2008).

Observations of polar coronal hole flows from *Ulysses*' third orbit showed characteristic differences in the solar wind compared to the previous solar cycle. The fast wind was slightly slower and significantly less dense, cooler, and had less mass and momentum flux than during the previous solar minimum (McComas et al. 2008). The reduction in the ram pressure of ~20% appears well correlated with the ~25% reduction in the open flux and measurements in the slower, ecliptic wind indicate essentially identical trends. Therefore, the changes in *Ulysses*' third orbit represent significant, long-term variations in solar wind output from the entire Sun. The observations indicate a reduction in the mass and energy fed into the wind below the sonic point (Leer & Holzer 1980). In this context, Schwadron & McComas (2003) provided a model for the source of solar wind energy and matter that may naturally explain the *Ulysses*' third orbit observations.

The Schwadron & McComas (2003) "scaling law" model provided a possible explanation for the fact that the speed of the solar wind observed in situ in interplanetary space is anticorrelated with its coronal freezing-in temperature (Geiss et al. 1995, Fig. 2; von Steiger et al. 2000, Fig. 6), which is

[1] Boston University, Department of Astronomy, Boston, MA 02215.
[2] Southwest Research Institute, San Antonio, TX 78228.

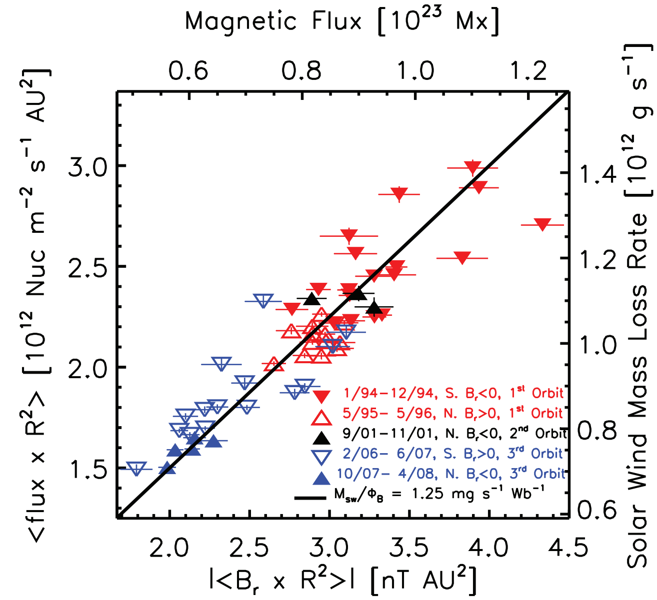

FIG. 1.—Solar wind mass flux vs. the magnitude of the magnetic flux density, $|\langle\bar{B}\rangle|$, in the *Ulysses* polar regions for latitudes above $\pm 40°$ and for solar wind speeds >710 km s^{-1}. We have included the solar wind He^{++} flux in these estimates. The left-hand vertical scale shows the radially normalized average mass flux, while the right-hand scale multiplies by the area of a sphere at 1 AU to form the total mass-loss rate. Similarly, the lower horizontal scale applies to the magnetic flux density, while the upper scale applies to the total magnetic flux. The black line from the model of Schwadron & McComas (2003) model with a mass-loss rate per magnetic flux of 1.25 mg s^{-1} Wb^{-1} matches the observations remarkably well.

determined from the charge state distributions of heavy elements. The freezing-in temperature is set low in the corona, where the solar wind draws ions out faster than they can equilibrate (through ionization and recombination) to the local electron temperature. One explanation for this anticorrelation is based on a reduction of the Aflvén speed in the sources of slow wind from larger and hotter coronal loops (Fisk 2003; Gloeckler et al. 2003). Instead, Schwadron & McComas (2003) suggested that the anticorrelation results if both fast and slow solar winds arise from the same small-scale structures that inject a roughly fixed electromagnetic energy per particle, $m\bar{v}_a^2$, but that a slow solar wind radiates more energy due to higher coronal temperatures. The roughly fixed injected electromagnetic energy per particle leads to a well-organized final solar wind speed. The physical principles behind the model have been well known for three decades: the strong dependence of the solar wind speed on coronal temperature is due to coronal heat conduction, which sets pressure in loops (Rosner et al. 1978), the inner boundary conditions, and many properties of the solar wind (e.g., Hammer 1982; Leer et al. 1982). In regions where conductive and radiative losses are insignificant, the final wind speed achieves its maximum steady state value of ~800 km s^{-1}, $mu_{\max}^2/2 = m\bar{v}_a^2 - GM_\odot m/R_\odot$, and the coronal source temperature is cool, as observed in coronal holes. (This expression was also derived by Fisk et al. [1999] by relating magnetohydrodynamic Poynting and mass flux to the emergence of new magnetic flux on the Sun.) In contrast to the fast wind, a slow wind is formed from hotter and brighter regions, where heat conduction funnels more energy into radiative loss in the chromosphere. The Schwadron & McComas (2003) model requires an energy flux, $\bar{Q}_0$, from small-scale structures that is given by $\bar{Q}_0 = (mu_{\max}^2/2 + GM_\odot m/R_\odot) f_0$ where f_0 is the base particle flux. The power needed for this solar wind source is derived by multiplying by the area, A_0, on the Sun covered by open flux, $P_{\rm sw} = (mu_{\max}^2/2 + GM_\odot m/R_\odot)\dot{N}_{\rm sw}$, where $\dot{N}_{\rm sw} = f_0 A_0$ is the ion transfer rate into the open flux region. We argued that the base flux, f_0, must be proportional to the base open flux, since observations show that the particle flux is relatively constant despite the large variability of field strengths at the source of solar wind; in this case, the particle flux at 1 AU is given by $f_1 = f_0(B_{1r}/B_0)$, where B_0 is the base field strength of the open field and B_{1r} is the radial field strength referenced to 1 AU. The flux relation applies since both particle and magnetic flux are conserved along magnetic flux tubes. With the particle flux relation, we derive the solar wind power in terms of the open flux, Φ_B, $P_{\rm sw} = [(mu_{\max}^2/2 + GM_\odot m/R_\odot)(f_1/B_{1r})]\Phi_B$, which shows that the maximum power of the solar wind (e.g., the fast solar wind power) will scale with the open magnetic flux.

Presumably, if the argument holds that maximum power in the solar wind scales with the open flux, then the power available for coronal heating should also scale with magnetic flux. Schwadron et al. (2006) made the direct comparison between solar wind power and coronal heating by deriving the fraction of total power (~1%) that goes into X-ray luminosity from closed magnetic structures on the Sun. The resulting comparison between the solar wind power and X-ray luminosity due to coronal heating revealed a consistent, almost linear, scaling between power or luminosity and magnetic flux, as demonstrated by Pevtsov et al. (2003). In particular, the X-ray luminosity scales with magnetic flux to the power of 1.2, which Schwadron et al. (2006) showed is consistent with the solar wind power both in its proportion to magnetic flux and in total magnitude.

This Letter studies the relationship between the observed solar wind power and total open magnetic flux as they respond to the changes in the Sun between *Ulysses*' first and third orbits.

2. OBSERVATIONS

Assuming fast wind approaches the maximum wind speed, the *Ulysses* measurements of flux, nu, and energy flux, ρu^3, allow us to characterize the source power per magnetic flux that energizes the solar wind,

$$\frac{\langle P_{\rm sw}\rangle}{|\langle\Phi_B\rangle|} = \frac{1}{2}\,\frac{\langle\rho u^3 R^2\rangle}{|\langle\bar{B}R^2\rangle|} + \frac{GM_\odot}{R_\odot}\,\frac{\langle\dot{M}_{\rm sw}\rangle}{|\langle\Phi_B\rangle|}\,, \quad (1)$$

where n is ion density, ρ is mass density, u is the solar wind speed, R is radial distance, $\dot{M}_{\rm sw}$ is the solar wind mass-loss rate, and the magnetic flux density is $\bar{B} = \Phi_B/A$, which is approximately the radial component of the magnetic field, B_r.

The model of Schwadron & McComas (2003) has a fixed injection of energy-per-particle in the fastest solar wind, and a mass flux proportional to magnetic flux. If these inferences hold then both the energy flux over magnetic flux density, $0.5\langle\rho u^3R^2\rangle/|\langle\bar{B}R^2\rangle|$, and the mass flux over magnetic flux density, $\langle\rho uR^2\rangle/|\langle\bar{B}R^2\rangle| = \langle\dot{M}_{\rm sw}\rangle/|\langle\Phi_B\rangle|$, should be constants in the fastest steady solar wind. Figure 1 tests these relationships by showing the mass flux versus the magnitude of the magnetic flux density, $|\langle\bar{B}\rangle|$, in the polar regions. The downward (upward) triangles indicate averages formed when *Ulysses* was in the southern (northern) hemisphere, while the open (closed) symbols indicate outward (inward) magnetic flux. The red, black, and blue data points were taken during *Ulysses* first, second, and third polar orbits, respectively. The time averages have been formed over 26 days and the bars on the data points

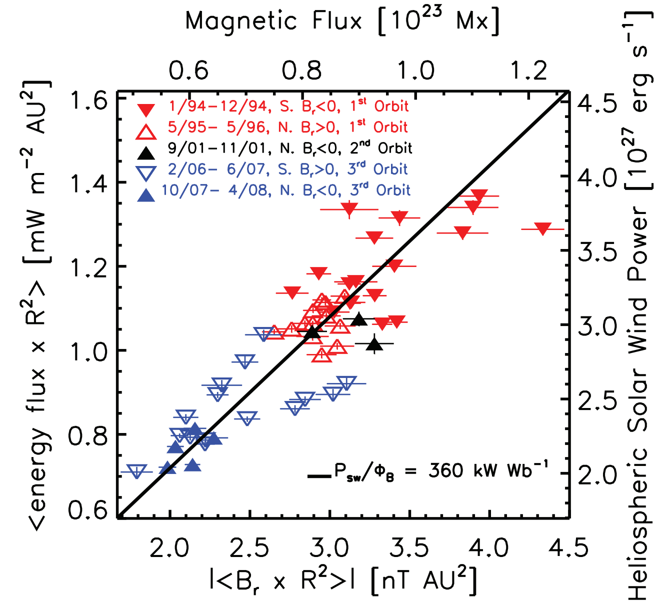

FIG. 2.—Solar wind energy flux $\langle \rho u^3 R^2 \rangle/2$ vs. $|\langle \bar{B} R^2 \rangle|$ using a format and an averaging process that is almost identical to that used for Fig. 1. The right-hand vertical scale shows the power of the solar wind after the gravitational potential of the particles has been lost. As in Fig. 1, the line from the Schwadron & McComas (2003) model has a power per magnetic flux of 360 kW Wb^{-1}.

show standard deviations of the mean values. The data shown include only nominal fast solar wind; a number of high-latitude coronal mass ejections (CMEs) observed near the beginning of 1994 (Schwadron et al. 1999) have been removed. The line is from the model of Schwadron & McComas (2003) model with a mass-loss rate per magnetic flux of 1.25 mg s^{-1} Wb^{-1}. The average magnetic flux density was derived directly from the radial component of the magnetic field, $|\langle \bar{B} R^2 \rangle| \approx |\langle B_r R^2 \rangle|$.

Figure 2 shows the solar wind energy flux $\langle \rho u^3 R^2 \rangle/2$ versus the unsigned magnetic flux density $|\langle \bar{B} R^2 \rangle|$ using a format and an averaging process that is almost identical to that used for Figure 1. As in Figure 1, the Schwadron & McComas (2003) model (*solid line*) matches the observations.

The top panel of Figure 3 combines the mass flux and energy flux averages to form the source solar wind power, as expressed in equation (1). The left-hand vertical scale shows source energy flux from the Sun needed to power the solar wind, and the right vertical scale shows the total power integrated over all solar wind sources. Again the linear scaling between power and magnetic flux is shown by the solid black line with a slope of 600 kW Wb^{-1}. The bottom panel in the figure places our *Ulysses* observations in the context of the X-ray results of Pevtsov et al. (2003). The upper line is the same 600 kW Wb^{-1} as shown in the top panel. Schwadron et al. (2006) showed that the power in the X-ray window of the bolometric luminosity should be ~1% of the total solar wind power, assuming that all solar wind power is converted into coronal heating in closed magnetic structures at the Sun. The red line with slope 6 kW Wb^{-1} therefore applies to the X-ray luminosity.

Table 1 shows these averages of the solar wind power over magnetic flux, solar wind flux, and energy flux in the polar fast solar wind observed during *Ulysses*' first through third orbits. Based on these values, we find $\langle \rho u^3 R^2 \rangle / (2|\langle \bar{B} R^2 \rangle|) =$ 360 ± 20 kW Wb^{-1}, $\dot{M}_{sw}/|\langle \Phi_B \rangle| = 1.25 \pm 0.06$ mg s^{-1} Wb^{-1}, and $\langle P_{sw} \rangle / |\langle \Phi_B \rangle| = 590 \pm 40$ kW Wb^{-1}.

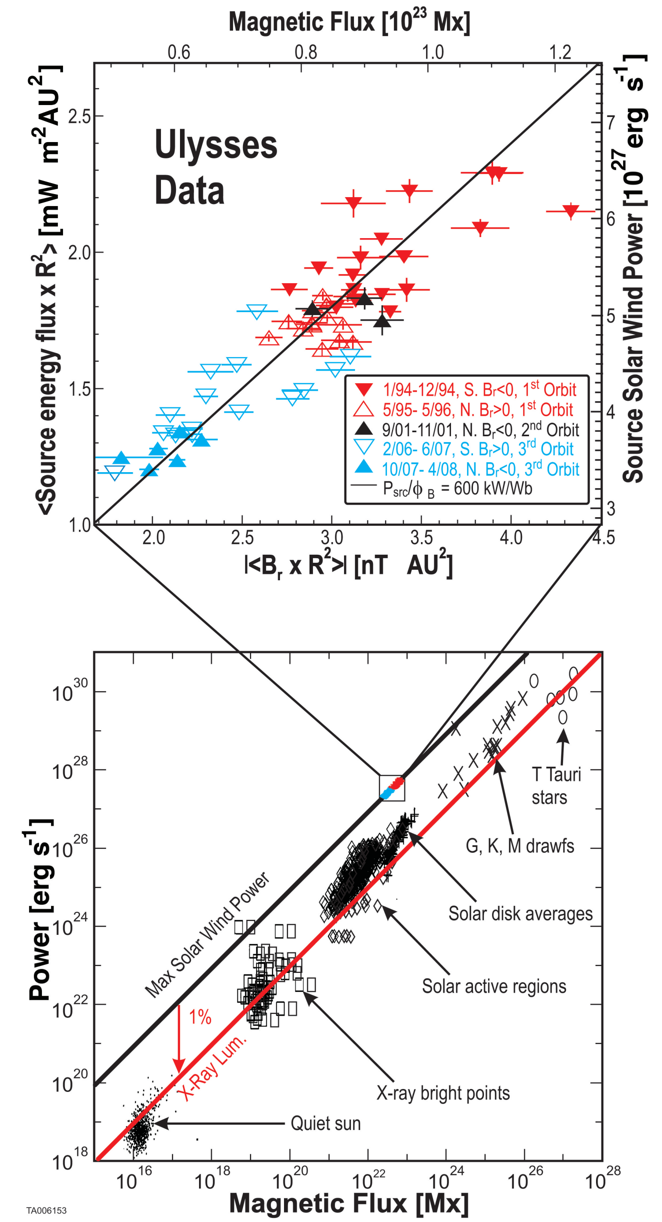

FIG. 3.—*Top*: Source solar wind power derived from the particle flux and energy flux averages, eq. (1). The linear scaling between power and magnetic flux (*solid black line*; Schwadron & McComas 2003) agrees well with the data. *Bottom*: Observations reported here in the context of the X-ray results of Pevtsov et al. (2003). The upper black line is the same 600 kW Wb^{-1} as shown in the top panel, and the lower red line shows the power in the X-ray window of the bolometric luminosity, about 1% of the total solar wind power (Schwadron et al. 2006).

Many models of the solar wind invoke the expansion properties of the open field to explain how the solar wind's final properties are determined (e.g., Wang & Sheeley 1990; Cranmer et al. 2007). Some models predict that the particle flux is approximately conserved at a given distance, while larger expansion in magnetic flux tubes should cause a slow-down in the solar wind. Observations of the Wilcox Solar Observatory show that there was a larger reduction (approximately a factor of 2) in the photospheric field strengths in coronal holes in the current solar minimum as compared to the previous cycle 22 solar minimum (Svalgaard & Cliver 2007). The reduction in the strength of the coronal hole fields is much larger than the

TABLE 1
AVERAGE PROPERTIES OF SOLAR WIND, POWER OVER MAGNETIC FLUX, MAGNETIC FLUX DENSITY, SOLAR WIND ENERGY FLUX, SOLAR WIND ION FLUX, AND THEIR FIELD WEIGHTED AVERAGES

Period	$\langle \bar{B}R^2 \rangle$ (nT)	$\langle \rho u^3 R^2 \rangle /2$ (mW m^{-2})	$\langle \rho u R^2 \rangle /m_p$ (10^{12} nucleons m^{-2} s^{-1})	$\langle \rho u^3 R^2 \rangle /(2 \lvert \langle \bar{B}R^2 \rangle \rvert)$ (kW Wb^{-1})	$\dot{M}_{sw} / \lvert \langle \Phi_B \rangle \rvert$ (mg s^{-1} Wb^{-1})	$\langle P_{sw} \rangle / \lvert \langle \Phi_B \rangle \rvert$ (kW Wb^{-1})
Orb. 1 (S), 93/10/7–95/1/19	−3.4 ± 0.1	1.20 ± 0.03	2.50 ± 0.06	360 ± 20	1.24 ± 0.06	590 ± 40
Orb. 1 (N), 95/5/3–96/5/1	2.94 ± 0.09	1.06 ± 0.01	2.43 ± 0.02	360 ± 10	1.21 ± 0.04	590 ± 30
Orb. 2 (N), 01/9/2–01/11/19	−3.1 ± 0.2	1.05 ± 0.03	2.34 ± 0.04	340 ± 20	1.25 ± 0.07	570 ± 40
Orb. 3 (S), 06/2/27–07/6/10	2.4 ± 0.1	0.86 ± 0.02	1.86 ± 0.06	360 ± 20	1.28 ± 0.08	600 ± 50
Orb. 3 (N), 07/10/18–08/4/1	−2.1 ± 0.08	0.76 ± 0.02	1.59 ± 0.03	360 ± 20	1.26 ± 0.05	600 ± 40

~30% reduction in the heliospheric field. Therefore, the overall expansion of the magnetic field must be smaller in the current cycle 23 than in the previous cycle. Such expansion models would predict a more powerful wind in the current compared to the previous solar minimum, which is the opposite of what *Ulysses* observes. However, there are models that contain a variation of magnetic flux at the lower boundary that can act in concert with the flux-tube expansion at larger distances (e.g., Wang 1995); this opens the question of whether expansion effects can in fact explain our observed correlation between mass flux, solar wind power, and magnetic flux.

3. DISCUSSION

Leer & Holzer (1980) examined the effects of solar wind heating and acceleration inside and outside the sonic point. The addition of energy above the sonic point primarily increases the wind speed whereas energy addition below the sonic point increases the mass and momentum flux proportionally, leading to little change in the final wind speed, but instead, a larger final particle and energy flux. McComas et al. (2008) therefore attributed the changes in the solar wind fluxes observed by *Ulysses* in the third orbit to reduced mass and energy fed in to the solar wind below the sonic point.

In the model of Schwadron & McComas (2003) the maximum power in the solar wind scales with the open magnetic flux. Schwadron et al. (2006) showed that this scaling is consistent with X-ray observations on the Sun also indicating an almost linear scaling between X-ray luminosity and magnetic flux (Pevtsov et al. 2003). Remarkably, the Pevtsov et al. (2003) observations include not only magnetic features on the Sun, but also other convective stars, which suggests that a universal property of magnetized plasmas may have been discovered.

The *Ulysses* observations show that solar wind energy flux is reduced by 27% and the particle flux is reduced by 30% in the third orbit as compared to the first orbit. These variations are roughly consistent with the 30% reduction of magnetic flux density observed in the third orbit. Further, the same north-to-south asymmetries observed in magnetic flux are also observed in particle flux and energy flux. These observations strongly support the linear scaling of solar wind power and particle flux with magnetic flux.

The *Ulysses* observations beg a deeper question of what regulates the power and mass input? Schwadron & McComas (2003) argue that the reconfiguration of the open magnetic field through the emergence of new magnetic flux regulates the energy-per-particle and mass flux injected into the solar wind. The emergence of new magnetic flux is likely controlled by convective processes.

The agreement between the *Ulysses* observations and the Pevtsov et al. (2003) X-ray results suggests that the Sun may be typical of other stars. The power of stellar winds should scale with the magnetic flux of the large-scale stellar fields. By observing astrospheres (e.g., Wood et al. 2005), and inferring the properties of their winds, the power versus magnetic flux scaling provides a way to also infer the large-scale magnetic fields generated by those stars, which places constraints on stellar dynamos.

In this study we have shown that the power of solar wind is regulated by the amount of magnetic flux that opens into the heliosphere. This places a new and stringent requirement that all solar wind models must satisfy. Finding this relationship on the Sun and a very similar one for X-ray emissions from other stars begs the question, does the wind power to magnetic flux constant (~600 kW Wb^{-1}) apply in general for convective stars?

REFERENCES

Babcock, H. W. 1961, ApJ, 133, 572
Cranmer, S. R., van Ballegooijen, A. A., & Edgar, R. J. 2007, ApJS, 171, 520
Fisk, L. A. 2003, J. Geophys. Res., 108, 1157, doi:10.1029/2002JA009284
Fisk, L. A., & Schwadron, N. A. 2001, ApJ, 560, 425
Fisk, L. A., Schwadron, N. A., & Zurbuchen, T. H. 1999, J. Geophys. Res., 104, 19765
Geiss, J., et al. 1995, Science, 268, 1033
Gloeckler, G., et al. 2003, J. Geophys. Res., 108, 1158, doi:10.1029/2002JA009286
Hammer, R. 1982, ApJ, 259, 779
Leer, E., & Holzer, T. E. 1980, J. Geophys. Res., 85, 4681
Leer, E., Holzer, T. E., & Fla, T. 1982, Space Sci. Rev., 33, 161
McComas, D. J., et al. 1998, Geophys. Res. Lett., 25, 1
———. 2000, J. Geophys. Res., 105, 10419
———. 2003, Geophys. Res. Lett., 30, 1517
———. 2008, Geophys. Res. Lett., 35, in press, doi:10.1029/2008GL034896
Owens, M. J., et al. 2007, Geophys. Res. Lett., 34, 6104
Pevtsov, A. A., et al. 2003, ApJ, 598, 1387
Rosner, R., Tucker, W. H., & Vaiana, G. S. 1978, ApJ, 220, 643
Schatten, K. H., Wilcox, J. M., & Ness, N. F. 1969, Sol. Phys., 6, 442
Schwadron, N. A., & McComas, D. J. 2003, ApJ, 599, 1395
Schwadron, N. A., McComas, D. J., & DeForest, C. 2006, ApJ, 642, 1173
Schwadron, N. A., et al. 1999, J. Geophys. Res., 104, 535
———. 2008, Ap&SS Trans., 4, 19
Smith, E. J., & Balogh, A. 2003, in AIP Conf. Proc. 679, Solar Wind Ten, ed. M. Velli, R. Bruno, F. Malara, & B. Bucci (New York: AIP), 67
———. 2008, Geophys. Res. Lett., in press
Svalgaard, L., & Cliver, E. W. 2007, ApJ, 661, L203
von Steiger, R., et al. 2000, J. Geophys. Res., 105, 27217
Wang, Y., & Sheeley, Jr., N. R. 1990, ApJ, 355, 726
Wang, Y.-M. 1995, ApJ, 449, L157
Wang, Y.-M., et al. 2002, J. Geophys. Res. Space Phys., 107, 1465
Wood, B. E., et al. 2005, ApJS, 159, 118